Chalcogenide Letters Vol. 19, No. 10, October 2022, p. 683 - 689

Chalcogenide glassy semiconductors of the system As-Se-S doped by Te for X-ray imaging

A. Chirita*, D. Spoiala, S.Vatavu
Semiconductors Physics and Devices Laboratory, Physics and Engineering Faculty, Moldova State University, Chisinau, Republic of Moldova

The polymer/ As-Se-S-Te structure for X-ray imaging has been investigated. The possibility of registering relief-phase images for radiation of "white" spectrum and λ=0,154 nm of *Cu* anode X-ray tube was shown.

(Received July 14, 2022; Accepted October 4, 20222)

Keywords: X-ray imaging, Chalcogenide glassy semiconductors, Thermoplastic

1. Introduction

A wide range of carriers and methods for recording optical information was developed and studied based on the chalcogenide glassy semiconductors (CGS) of the system As-Se-S. The photo-thermoplastic carriers, based on CGS, for real-time holography [1] have high values of resolution power - up to 4000mm^{-1} [2], diffraction efficiency - up to 40% [3], and the time of the image formation 1–3 s [4]. CGS are sensitive materials to electron-beam recording [5-7], photoinducted transformation (photodarkening, photorefraction) [8-10], and as photoresist materials sensitive in UV-visible regions [11]. The surface relief formation (mass-transport effect) in the glassy materials of the system As-Se-S under laser illumination was studied in works [12-13]. The As_2S_3 thin films, as photoresists for x-ray photolithography, were studied in works [14-15]. The maximum sensitivity of As_2S_3 for X-ray photolithography is in the spectral range λ=2-7 nm [14]. In [15], As_2S_3 thin films were studied as photoresists in the wavelength range λ=0,1-0,6nm, where their sensitivity is lower and large exposures are required. X-ray imaging studies using the polymer/As-Se-S-Sn structure are presented in work [16], which shows the sensitivity of As-Se-S-Sn to X-rays λ=0,154nm. This work aimed to study chalcogenide glassy semiconductors of the system As-Se-S doped by Te for x-ray imaging.

2. Experimental setup

The carriers for X-ray imaging were obtained as a multilayer structure (Fig.1a): the flexible polyethylene terephthalate film (PET) substrate (1) was covered with a semitransparent chrome electrode (2), the sensitive layer (3) based on $(As_2Se_3)_{0,8}(As_2S_3)_{0,188}Te_{0,012}$ with a thickness of 3,5μm was deposited onto the metal electrode by vacuum thermal deposition [17], and the thermoplastic layer of butilmetacrylate-styrene (4) with a thickness of 0,6 μm was deposited on the semiconductor layer.

* Corresponding author: arc_chirita@yahoo.com
https://doi.org/10.15251/CL.2022.1910.683

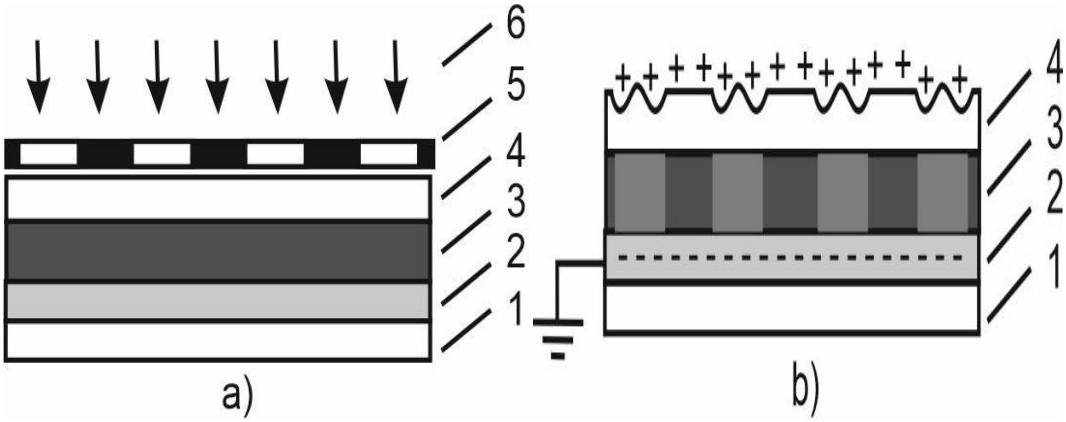

Fig. 1. (a) 1.Polyethylene terephthalate film, 2. Chrome electrode, 3.Semiconductor layer, 4. Thermoplastic polymer, 5. Brass mesh, 6. X-ray beam; (b) Visualization of recorded image.

The X-ray installation based on a tube with a copper anode (voltage 45 kV, current 40 mA) was used for irradiating the samples. The samples were studied under two types of irradiation: the copper anode tube spectrum without any filters (the continuous spectrum of X-ray, or "white" spectrum near to λ~0,027-0,25 nm) and a parallel X-ray beam close to the monochromatic wavelength of λ=0,154 nm. The monochromatic laser radiation λ=632,8nm was used for registration in the visible region of the spectrum. A brass mesh was used as a mask for x-ray image recording. The mask was placed onto the surface of the thermoplastic layer (5, Fig.1a) and irradiated with visible or X-ray irradiation (6). Unlike the photothermoplastic process, when illumination and registration are carried out simultaneously [18], the carrier is removed from the X-ray chamber after irradiation for the next step of image visualization [16, 19]. After irradiation the carrier is heated up to a vicious state of the thermoplastic layer ($T=68^0C$) in darkness and charged for 1,8-2,5 s with a high voltage (7,7 kV) corona charging (Fig.1b) [16]. The surface of the thermoplastic layer is charged with positive air ions (Fig.1b). The conductivity of the semiconductor layer in the irradiated areas is higher due to the change of resistivity under irradiation [16, 19]. Positive charges on the surface and negative charges in the semiconductor layer deform the thermoplastic under the Coulomb interaction [1] and a relief-phase image of the registered object is formed [4].

3. Results

Fig.2a shows the zoomed image of the brass mesh that was used as a mask (5, Fig.1). The images were recorded using the continuous spectrum of X-rays. The X-ray beam size was 5x20mm. Thermoplastic visualization (Fig.1b) was carried out at temperature $T=68^0C$ and charging time t=1,8s. After the visualization, the images were studied on an optical microscope in reflected light.

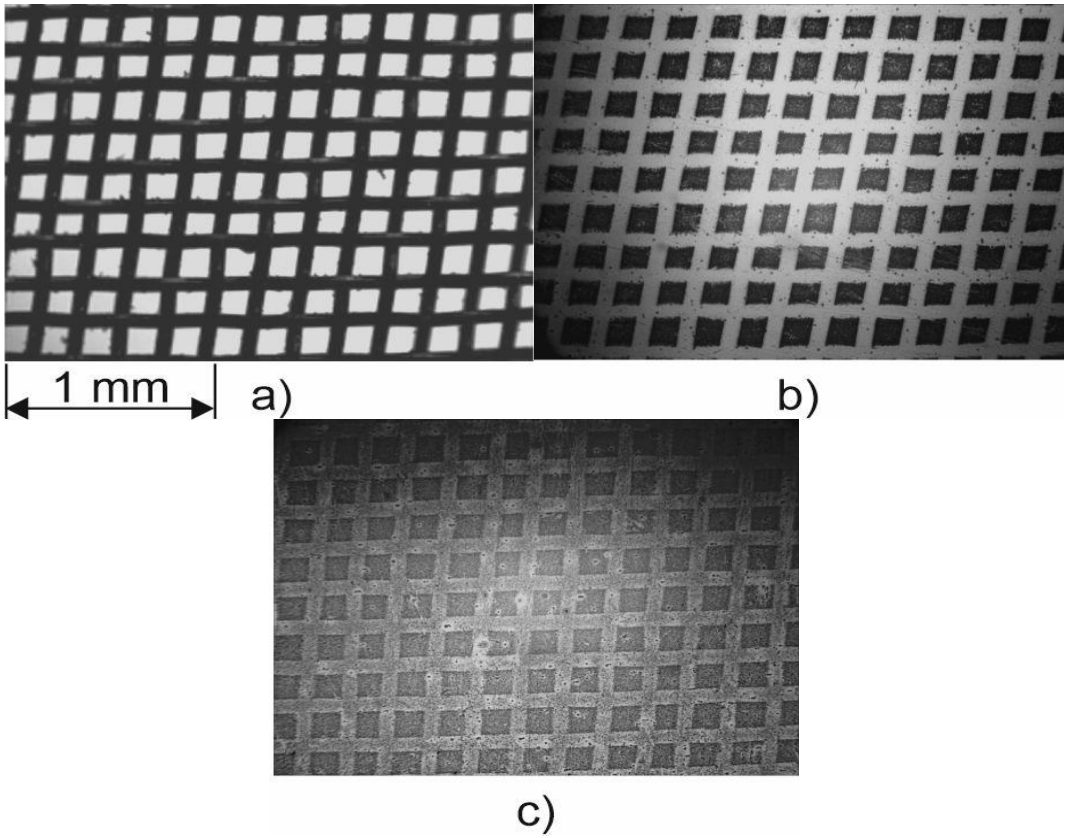

Fig. 2. (a) The brass mesh, used as a mask, b) X-ray image recorded at absorbed dose of 1,6 Gy, (c) X-ray image recorded at absorbed dose of 0,64 Gy.

Fig. 2b shows the image of a brass mesh obtained at an absorbed dose of 1,6Gy. As shown in Fig.2b, the thermoplastic process forms a negative image of the initial object, due to the deformation of the thermoplastic layer in irradiated areas. The following experiments were carried out with a decrease of the absorbed dose to the minimum sensitivity of the studied carriers. Fig.2c shows the image of a brass mesh obtained at an absorbed dose of 0,64 Gy and charging time t=2,5 s. The image shows an increase of noise in both irradiated and non-irradiated areas. The image has low contrast, but it is still possible to distinguish the outlines of the initial object on the registered image.

The following experiments were carried out with a parallel X-ray beam close to the monochromatic wavelength of λ=0,154 nm. Fig.3a shows an image of a brass mesh obtained at an X-ray exposure of 24,6 J/cm^2. Thermoplastic visualization (Fig.1b) was carried out at temperature T=68^{0}C, voltage 7,7 kV, and charging time t=1,8 s. Fig.3b (the top of the image) shows the edge of one of the squares of the mesh obtained at an optical magnification of 1200^X. A part of the image (a black square with an arrow) was investigated using the AFM. The selected part of the image covers both irradiated and non-irradiated areas.

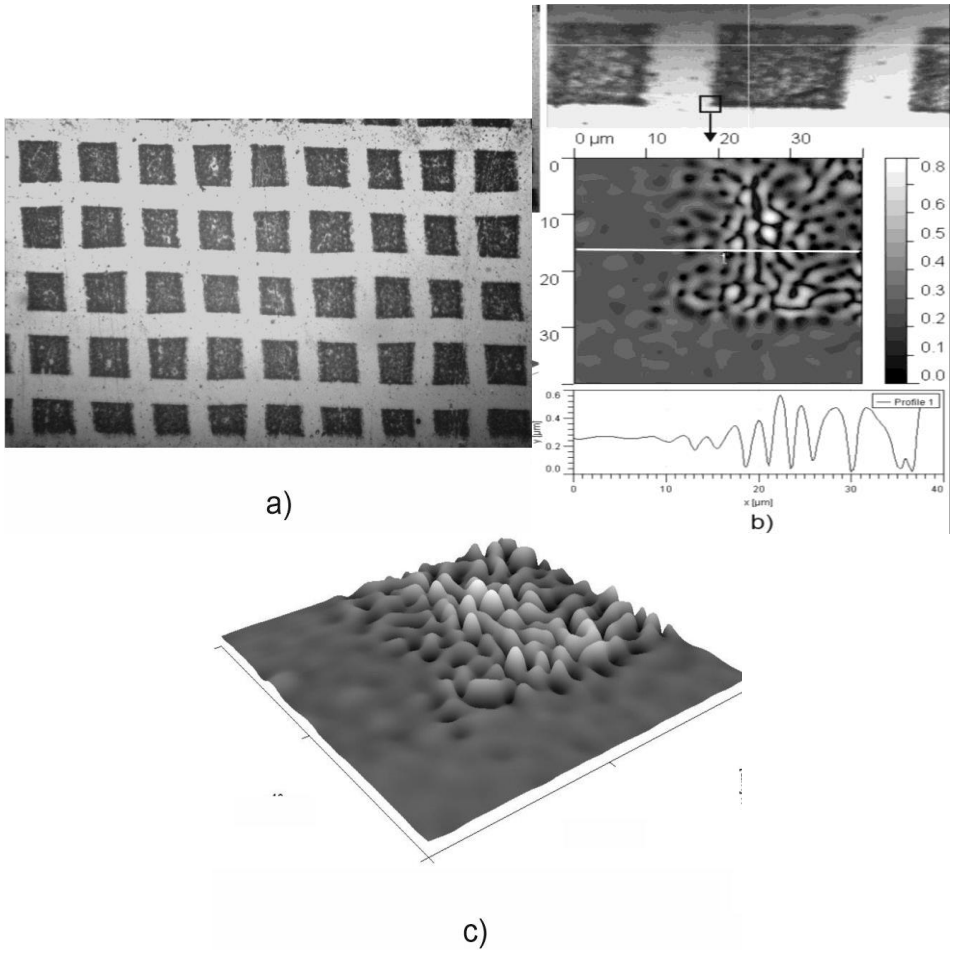

Fig. 3. (a) X-ray image recorded at exposure of 24,6 J/cm^2, (b) AFM image, (c) 3D image.

The AFM image of the selected area shows the presence of deformation of the thermoplastic layer in the irradiated areas and the absence of deformation in the non-irradiated ones. The surface profile (longitudinal white line along the image) shows the presence of depressions with a middle wide of about 1µm and with middle deep of about 0,4 µm at the exposed place (Fig.3b). Fig.3c shows a three-dimensional image of the selected area with deformation in the irradiated areas and no deformation in the non-irradiated ones. The following experiments were carried out with a decrease of the exposure to the minimum sensitivity of the carriers. Fig.4a shows an image of a brass mesh obtained at an X-ray exposure of 17,2 J/cm^2. Thermoplastic visualization was carried out at temperature T=68^{0}C, voltage 7,7 kV, and charging time t=2,5 s. Fig.4b (the top of the image) shows the edge of one of the squares of the mesh obtained at an optical magnification of 1200^X.

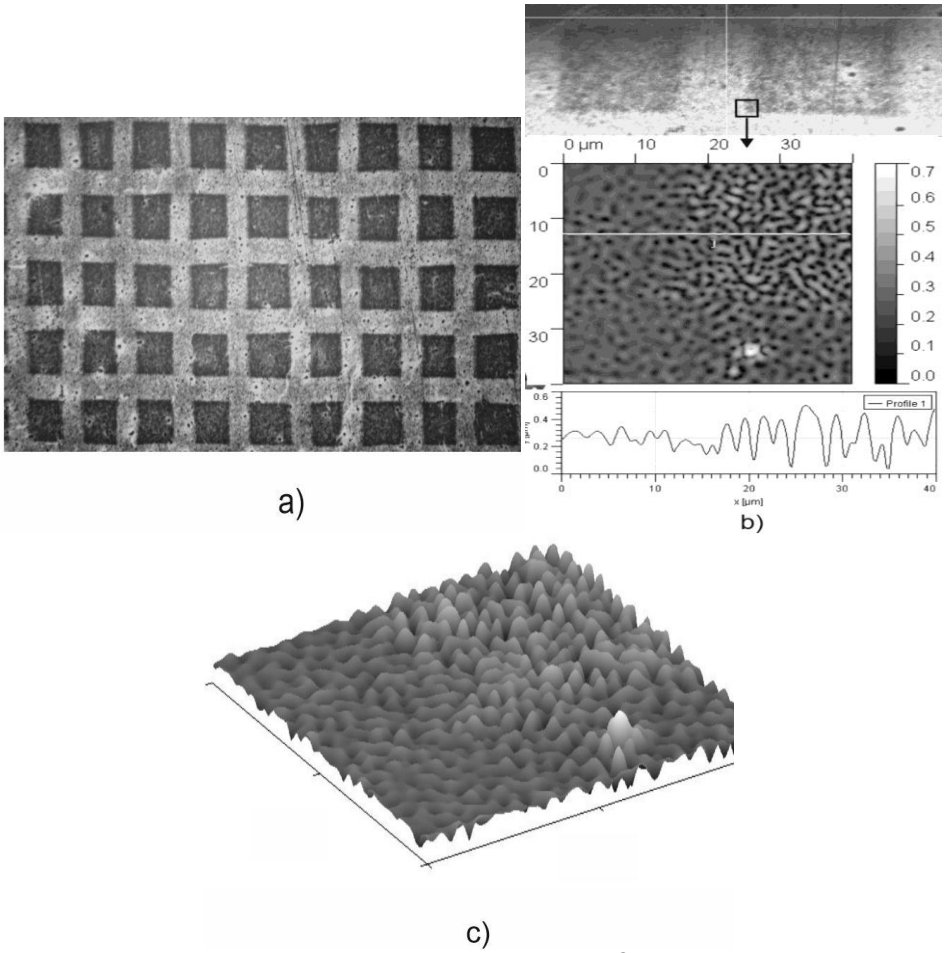

Fig. 4. (a) X-ray image recorded at exposure of 17,2 J/cm^2, b) AFM image, c) 3D image.

As can be seen from Fig.4b the increase of noise is observed both in the irradiated and non-irradiated areas of the image. A part of the image (a black square with an arrow) was investigated using the AFM. The selected part of the image covers both irradiated and non-irradiated areas. The AFM image of the selected area shows the presence of deformation of the thermoplastic layer both in the irradiated and non-irradiated areas. The surface profile (longitudinal white line along the image) shows the presence of depressions about 1µm wide and about 0,35 µm deep at the exposed place, and about 0,8 µm wide and about 0,12 µm deep at the non-irradiated areas (Fig.4b). Fig.4c shows a three-dimensional image of the selected area with deformation both in the irradiated and non-irradiated areas.

For comparison with X-rays, carriers were investigated for visible light imaging. Similar to the previous experiments, the carriers were illuminated through a mask with monochromatic radiation λ=632,8 nm at an intensity of 30m W/cm^2. Thermoplastic visualization was carried out under the same conditions as X-rays imaging. The images with a good contrast were obtained at an exposure power of 180 mJ/cm^2.

The effect of photostructural changes (photodarkening, photorefraction) in chalcogenide glassy semiconductors under optical radiation is well known from the bibliography sources [12, 20–21]. This effect was not observed during X-ray irradiation of the investigated carriers. For this research, a semiconductor layer was deposited on a sapphire substrate to exclude the effect of X-rays on the PET substrate. Measurement of the spectral dependence of transmission before and after X-ray irradiation at absorbed dose up to 1,6 Gy showed no change in the optical transmittance of the samples under study.

4. Discussions

The performed studies showed the sensitivity of the chalcogenide glassy semiconductors of the $(As_2Se_3)_{0,8}(As_2S_3)_{0,188}Te_{0,012}$ system to X-rays. The deformation of the thermoplastic layer in the irradiated areas takes place both under irradiation by a continuous spectrum of λ~0,027-0,25 nm, close to the monochromatic X-ray with the wavelength λ=0,154nm, and monochromatic laser radiation λ=632,8 nm. This indirectly indicates the presence of structural changes in the semiconductor layer under X-ray irradiation, which modulates the resistivity of the semiconductor layer [16,19]. However, no change in the optical transmittance in the $(As_2Se_3)_{0,8}(As_2S_3)_{0,188}Te_{0,012}$ layer under X-rays irradiation at an absorbed dose of 1,6 Gy (continuous spectrum λ~0,027-0,25 nm) and exposures up to 24,6 J/cm^2 (λ~0,154 nm) was detected. The same results were presented in work [16] for chalcogenide glassy semiconductors of the As-Se-S system doped by Sn. According to the investigations presented in works [22–23], a change in the optical properties of CGS was found under the γ-radiation. The darkening in the layers of As-S was observed upon irradiation with hard γ-quanta (1,25 MeV) and at high radiation doses - up to 10 MGy [22–23].

Based on the obtained results and on the results presented in [16], can be concluded that the structural changes in the semiconductor layer under the action of X-rays are very insignificant. However, even small changes in the resistivity of the semiconductor layer may be sufficient for thermoplastic visualization. The thermoplastic process is very sensitive due to the Coulomb interaction between the charges on the surface of the thermoplastic layer and the charges in the semiconductor layer [24-25].With an increase in the charging time to 2,5 s, even free charge carriers are sufficient for the appearance of noise deformation of the thermoplastic layer in non-irradiated places (Fig.4).

The sensitivity of the $(As_2Se_3)_{0,8}(As_2S_3)_{0,188}Te_{0,012}$ structure for X-ray recording is less than for As-Se-S structure doped by Sn [16]. However, the exposure interval for X-ray recording on the $(As_2Se_3)_{0,8}(As_2S_3)_{0,188}Te_{0,012}$ is 17,2–24,6 J/cm^2, which shows a higher sensitivity compared to X-ray lithography for the spectral range λ=0,1-0,6 nm [15]. As was shown in this work, the As_2S_3 thin films require exposures of 25–50 J/cm^2 in this wavelength range.

5. Conclusions

The carriers based on the polymer/$(As_2Se_3)_{0,8}(As_2S_3)_{0,188}Te_{0,012}$ structure make it possible to record images in the visible spectral range, using the continuous spectrum of an X-ray tube with the copper anode, and at a wavelength of 0,154 nm. Structural changes in semiconductors of the As-Se-S system under X-ray irradiation, such as a change of chemical etching in X-ray lithography [14-15] and thermoplastic visualization [16] require a detailed study, which was not the purpose of this work. At this stage, only experimental results on the registration of X-ray images are presented.

Chalcogenide glassy semiconductors are successfully used to record relief-phase holographic images with high diffraction efficiency [3, 24] and resolution power [25], so X-ray holography may be the most promising way to use these structures.

Acknowledgements

This research was funded by the National Agency for Research and Development of the Republic of Moldova, grant 20.80009.5007.12

References

[1] A. Chirita, N. Kukhtarev, T. Kukhtareva, O. Korshak, V. Prilepov, Journal of Modern Optics 59(16), 1428 (2012); https://doi.org/10.1080/09500340.2012.719936
[2] A. Chirita, N. Kukhtarev, T. Kukhtareva, O. Korshak, V. Prilepov, Laser Physics 23, 036002 (2013); https://doi.org/10.1088/1054-660X/23/3/036002
[3] I. Andries, T. Galstian, A. Chirita, J. Optoelectron. Adv. M. **18**(1-2), 56 (2016)
[4] A. Chirita, V. Prilepov, M. Popescu, I. Andries, M. Caraman, Iu. Jidcov, J. Optoelectron. Adv. M. **17**(7-8), 925 (2015)
[5] M. Iovu, S. Sergeev, O. Iaseniuc, Optoelectron. Adv. Mat. **12**(7-8), 377 (2018)
[6] O. Iaseniuc, M. Enachescu, D. Dinescu, M. Iovu, S. Sergheev, J. Optoelectron. Adv. M. **18**(1-2), 34 (2016)
[7] S. Sergeev, M. Iovu, A. Meshalkin, Chalcogenide Letters 17(1), 25 (2020)
[8] O. Iaseniuc, I. Cojocaru, A. Prisacar, A. Nastas, M. Iovu, Journal of Optics and Spectroscopy 121(1), 1128 (2016); https://doi.org/10.1134/S0030400X16070237
[9] A. Nastas, A. Andriesh, V. Bivol, A. Prisakar, G. Tridukh, Technical Physics Letters 32(1), 45 (2006); https://doi.org/10.1134/S1063785006010159
[10] A. Nastas, A. Andriesh, V. Bivol, A. Prisakar, G. Tridukh, Technical Physics 54(2), 305 (2009); https://doi.org/10.1134/S1063784209020236
[11] J. Teteris, M. Reinfelde, Journal of Optoelectronics and Advanced Materials 5(5), 1355 (2003)
[12] E. Achimova, A. Stronski , V. Abaskin, A. Meshalkin, A. Paiuk, A. Prisacar, P. Oleksenko, G. Triduh, Optical Materials 47, 566 (2015); https://doi.org/10.1016/j.optmat.2015.06.044
[13] V. Cazac, A. Meshalkin, E. Achimova, V. Abashkin, V. Katkovnik, I. Shevkunov, D. Claus, and G. Pedrini, Applied Optics 57, 507 (2018); https://doi.org/10.1364/AO.57.000507
[14] G. Danev, E. Spassova, J. Assa, P. Guttmann, Advanced materials for optics and electronics 8, 129 (1998); https://doi.org/10.1002/(SICI)1099-0712(199805/06)8:3<129::AID-AMO331>3.0.CO;2-5
[15] A. Buroff, A. Rush, Journal of Non Crystalline Solids 90, 585 (1987); https://doi.org/10.1016/S0022-3093(87)80491-X
[16] A. Chirita, V. Prilepov. Chalcogenide Letters 19(6), 439 (2022)
[17] V. Prilepov, M. Popescu, A. Chirita, O. Korshak, P. Ketrush, N. Nasedchina. Chalcogenide Letters 10(7), 249 (2013)
[18] A. Chirita, V. Prilepov, M. Popescu, O. Corsac, P. Chetrus, N. Nasedchina. Optoelectron. Adv. Mat. **9**(7-8), 919 (2015).
[19] A.Nastas, A. Andriesh, V. Bivol, I. Slepnev, A. Prisakar, Technical Physics Letters 35(4), 375 (2009); https://doi.org/10.1134/S1063785009040269
[20] J. De Neufville, S. Moss, S. Ovshinsky, Journal of Non-Crystalline Solids 13, 191(1973); https://doi.org/10.1016/0022-3093(74)90091-X
[21] T. Uchino, D. Clary, Physical Review Letters 85(15), 3305 (2000); https://doi.org/10.1103/PhysRevLett.85.3305
[22] O. Shpotyuk, A. Matkovskii, Journal of Non-Crystalline Solids 176, 45 (1994); https://doi.org/10.1016/0022-3093(94)90209-7
[23] M. Shpotyuk, A. Kovalskiy, R. Golovchak, O. Shpotyuk, Journal of Non-Crystalline Solids 498, 315 (2018); https://doi.org/10.1016/j.jnoncrysol.2018.04.006
[24] A. Chirita, T. Galstian, M. Caraman, V. Prilepov, O. Korshak, I. Andries, Optoelectron. Adv. Mat. **7**(3-4), 293 (2013)
[25] A. Chirita, F. Dimov, S. Pradhan, P. Bumacod, O. Korshak, Journal of Nanoelectronics and Optoelectronics 7(4), 415 (2012); https://doi.org/10.1166/jno.2012.1321